

LETTER TO THE EDITOR

The dust content of high- z submillimeter galaxies revealed by *Herschel* [★]

P. Santini¹, R. Maiolino¹, B. Magnelli², L. Silva³, A. Grazian¹, B. Altieri⁴, P. Andreani^{3,5}, H. Aussel⁶, S. Berta², A. Bongiovanni^{7,8}, D. Brisbin⁹, F. Calura^{3,10}, A. Cava^{7,8}, J. Cepa^{7,8}, A. Cimatti¹¹, E. Daddi⁶, H. Dannerbauer⁶, H. Dominguez-Sanchez¹², D. Elbaz⁶, A. Fontana¹, N. Förster Schreiber², R. Genzel², G. L. Granato³, C. Gruppioni¹², D. Lutz², G. Magdis⁶, M. Magliocchetti¹³, F. Matteucci¹⁴, R. Nordon², I. Pérez García⁴, A. Poglitsch², P. Popesso², F. Pozzi¹¹, L. Riguccini⁶, G. Rodighiero¹⁵, A. Saintonge², M. Sanchez-Portal², L. Shao², E. Sturm², L. Tacconi², and I. Valtchanov²

(See online Appendix A for author affiliations)

Received ; accepted

ABSTRACT

We use deep observations taken with the Photodetector Array Camera and Spectrometer (PACS), on board the *Herschel* satellite as part of the PACS evolutionary probe (PEP) guaranteed project along with submm ground-based observations to measure the dust mass of a sample of high- z submillimeter galaxies (SMGs). We investigate their dust content relative to their stellar and gas masses, and compare them with local star-forming galaxies. High- z SMGs are dust rich, i.e. they have higher dust-to-stellar mass ratios compared to local spiral galaxies (by a factor of 30) and also compared to local ultraluminous infrared galaxies (ULIRGs, by a factor of 6). This indicates that the large masses of gas typically hosted in SMGs have already been highly enriched with metals and dust. Indeed, for those SMGs whose gas mass is measured, we infer dust-to-gas ratios similar or higher than local spirals and ULIRGs. However, similarly to other strongly star-forming galaxies in the local Universe and at high- z , SMGs are characterized by gas metallicities *lower* (by a factor of a few) than local spirals, as inferred from their optical nebular lines, which are generally ascribed to infall of metal-poor gas. This is in contrast with the large dust content inferred from the far-IR and submm data. In short, the metallicity inferred from the dust mass is much higher (by more than an order of magnitude) than that inferred from the optical nebular lines. We discuss the possible explanations of this discrepancy and the possible implications for the investigation of the metallicity evolution at high- z .

Key words. Galaxies: evolution - Galaxies: high-redshift - Galaxies: ISM - Infrared: galaxies - Submillimeter: galaxies

1. Introduction

Understanding the evolution of the dust properties and the dust content of galaxies through the cosmic epochs is crucial for constraining galaxy evolutionary scenarios. The amount of dust has important implications for the star formation (SF). Dust allows the formation of low-mass stars in low-metallicity environments while it inhibits the formation of massive stars, hence affects the IMF (e.g. Omukai et al. 2005). Dust greatly enhances the formation of many molecules whose transitions provide the main cooling mechanism for molecular clouds to form stars. Hence dust is one of the pre-requisites for enhanced SF. Dust also affects the detectability of high- z galaxies: dust extinction reduces the detectability of high- z galaxies in the rest-frame UV-optical bands, while dust thermal emission allows the detection of high- z galaxies at mm/far-IR wavelengths. The dust content can also be used as a proxy of the metallicity of the ISM, because refractory elements in the ISM are mostly depleted into dust grains.

The ESA *Herschel* Space Observatory (Pilbratt et al. 2010) offers the possibility to investigate the dust emission in high- z star-forming galaxies and in particular to measure their dust content by modeling the far-IR to submm spectral energy dis-

tribution (SED). We here present a first investigation of dust mass evolution by focusing on a sample of high- z submillimeter galaxies (SMGs). They are very luminous ($\sim 10^{13} L_{\odot}$) (e.g., Hughes et al. 1998; Pope et al. 2006), high redshift ($z \sim 1-3.5$) (Chapman et al. 2005; Pope et al. 2006), gas rich and compact, massive galaxies (Greve et al. 2005; Tacconi et al. 2008). Their star formation rates (SFR) are exceptionally high ($\sim 10^3 M_{\odot} \text{yr}^{-1}$) and are thought to contribute significantly to the cosmic SF at $z \sim 2-3$ (Chapman et al. 2005). Thanks to their high luminosities they provide an excellent laboratory to investigate the evolution of dust in high- z galaxies. To measure their dust content we use data taken with PACS (Poglitsch et al. 2010) as part of the PACS Evolutionary Probe guaranteed time key program combined with ground-based mm and submm data. By comparing the inferred dust masses with other properties of the SMGs, and with local galaxies, we infer important information on the physics of these high- z systems. We adopt the Λ -CDM concordance cosmological model ($H_0 = 70 \text{ km/s/Mpc}$, $\Omega_M = 0.3$ and $\Omega_{\Lambda} = 0.7$).

2. Sample and data analysis

We used deep 100 and 160 μm PACS GTO observations of the field GOODS-N and of the lensing cluster Abell2218. Observations, data reduction and source extraction are described in detail in Berta et al. (2010). As mentioned above, we used a subset of PACS sources with submm detections taken from the literature. The SMG sample and counterparts association

Send offprint requests to: P. Santini, e-mail: paola.santini@oa-roma.inaf.it

[★] *Herschel* is an ESA space observatory with science instruments provided by European-led Principal Investigator consortia and with important participation from NASA.

are described in Magnelli et al. (2010). The sample is restricted to sources with secure redshifts (all spectroscopic, except for three sources with good photo- z) derived from robust multi-wavelength associations. A few SMGs in the GOODS-N field have two optical, and eventually PACS, counterparts at the same redshift. For these we considered the total system of the two galaxies, which are likely interacting (Pope et al. 2006), by summing their IR fluxes and stellar masses. We excluded three galaxies (GN19, GN19b, GN30) with only two photometric points at $\lambda > 100\mu\text{m}$ because their SED could not be properly constrained. Finally, we excluded a galaxy (azt23) with a peculiar SED, suspected to be dominated by a powerful AGN even at far-IR wavelengths. We ended up with 12 SMGs in GOODS-N and 5 in Abell2218, three of the latter are different images of the same lensed galaxy. All our galaxies have PACS (100 and $160\mu\text{m}$) and SCUBA $850\mu\text{m}$ photometry, and nine also have SCUBA $450\mu\text{m}$ and/or AzTEC 1.1mm and/or MAMBO 1.2mm detections. Redshifts range from 0.5 to 4, with a median value of 2.

Both to expand the sample and to check that our dust masses are not subject to systematics associated with the specific set of data, we also included six SMG galaxies observed by Kovács et al. (2006) at $350\mu\text{m}$ with SharcII, which have at least two additional (sub)mm photometric points, and one MIPS (both 70 and $160\mu\text{m}$) detected SMG from the Yan et al. (2010) sample, with also a MAMBO 1.2mm observation.

Dust masses were derived by fitting and normalizing the $100\mu\text{m}$ -to-(sub)mm photometry to the SED library generated by GRASIL (Silva et al. 1998). This is a chemospectrophotometric code that uses realistic and physically grounded stellar and dust distributions and geometries and performs the full radiative transfer calculations, eventually providing the complete SED of various galaxy models. Recently, GRASIL has been convolved with models of dust evolution in galaxies (Calura et al. 2008; Schurer et al. 2009). The model carefully takes into account the different emissivities of different populations of dust grains, which also depend on their size, composition, and temperature. This effectively results in an average emissivity index $\beta \approx 2$, consistent with various previous studies (Silva et al. 1998; Draine & Li 2007; Clements et al. 2010). The dust masses inferred by us broadly agree with those obtained by Michałowski et al. (2010a), who also use GRASIL, although the lack of data at $24\mu\text{m} < \lambda < 850\mu\text{m}$ in most objects prevents them from tightly constraining the far-IR bump.

The inferred dust mass is compared with the stellar mass, gas mass, and gas metallicity as inferred for a subset of the objects in our total sample by ancillary data presented in the Appendix. We also compared the dust properties of SMGs with those of local star-forming galaxies, both spirals and ULIRGs, whose properties are reported in the Appendix. Here we only mention that the methods to derive the dust mass, stellar mass, gas mass, and metallicity are the same for all samples, so that their comparison is done in a fully consistent way.

3. Results and discussion

Figure 1 shows the stellar mass vs the dust mass for high- z SMGs (black circles), local ULIRGs (blue squares) and local spirals (red triangles). The dust masses estimated for local spirals nicely agree with those obtained through the very detailed analysis of Draine et al. (2007) of the same sample. Most of them also agree fairly well with the evolutionary pattern for spiral galaxies predicted by the model of Calura et al. (2008) (cyan solid line). The dust masses were compared with those obtained by the more common assumption of a single temperature dust distribu-

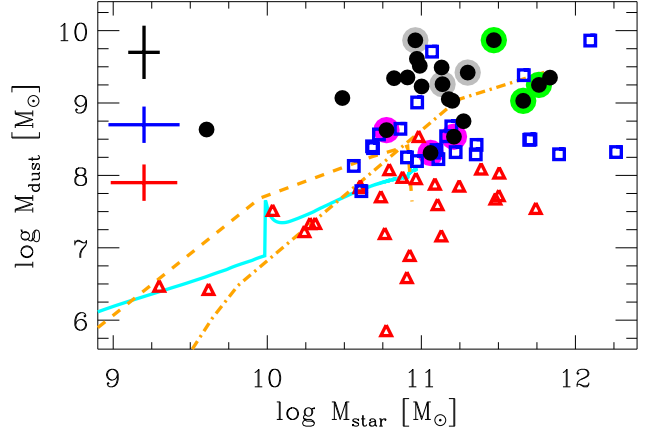


Fig. 1. Stellar mass versus dust mass. Blue squares show local ULIRGs, red triangles refer to local spirals, while black circles correspond to high- z SMGs. Large gray, magenta and green circles mark respectively photo- z , the triple image in Abell2218 and blended SMG systems. Median 1σ error bars for the different samples (same color code) are shown on the left. The solid cyan and dashed (dot-dashed) orange lines show the predictions of Calura et al. (2008) model for spirals and proto-ellipticals with mass of 10^{11} (10^{12}) M_{\odot} .

tion. Assuming an emissivity index $\beta = 2$ (for consistency with GRASIL) and a single, absolute average emissivity of dust at $125\mu\text{m}$ of 2.64 (Dunne et al. 2003) or $1.87\text{m}^2\text{kg}^{-1}$ (Li & Draine 2001), dust masses are on average 0.3 or 0.15 dex, respectively, lower than those inferred through GRASIL ($100\mu\text{m}$ flux not used in the fitting as in Magnelli et al. 2010). Independently of the adopted method, there are clear, systematic differences in terms of dust content for the different samples. The orange dashed and dot-dashed lines in Fig. 1 show the expected evolution of proto-ellipticals (Calura et al. 2008) with different mass. These models predict a larger dust content during the active phase of elliptical formation compared to normal spirals. Nonetheless, they can hardly reproduce the large $M_{\text{dust}}/M_{\text{star}}$ observed in most SMGs. The dust-to-star excess in SMGs emerges more clearly in Fig. 2a, which shows the distribution of $M_{\text{dust}}/M_{\text{star}}$ for the different samples. Local ULIRGs have a larger dust content than spirals for a given stellar mass, with $M_{\text{dust}}/M_{\text{star}}$ a factor of ~ 4 higher on average. This result is in contrast with Clements et al. (2010), who claimed that the dust content in ULIRGs can be simply explained with the combination of two spirals (the different result probably arises because Clements et al. use only K-band photometry as a proxy of the stellar mass, while we perform the full SED fitting). Submillimeter galaxies are much more extreme: their $M_{\text{dust}}/M_{\text{star}}$ is on average higher by a factor of ~ 30 than in local spirals, and by a factor of ~ 6 than in local ULIRGs. This large dust content is difficult to account for with the galaxy evolutionary model of Calura et al. (2008).

High- z SMGs are known to be very gas rich, with gas fractions approaching 50% (Tacconi et al. 2008). The high $M_{\text{dust}}/M_{\text{star}}$ values suggest that the large gas masses hosted by SMGs have already been highly enriched with metals and dust; i.e. the excess of dust mass in SMGs is not a consequence of SF episodes following recent inflows of metal-poor gas accreted during mergers (in contrast with the expectation of some models, Montuori et al. 2010). This can be tested by measuring the dust-to-gas ratio for those SMGs with CO millimetric data. By assuming the same CO-to- H_2 conversion

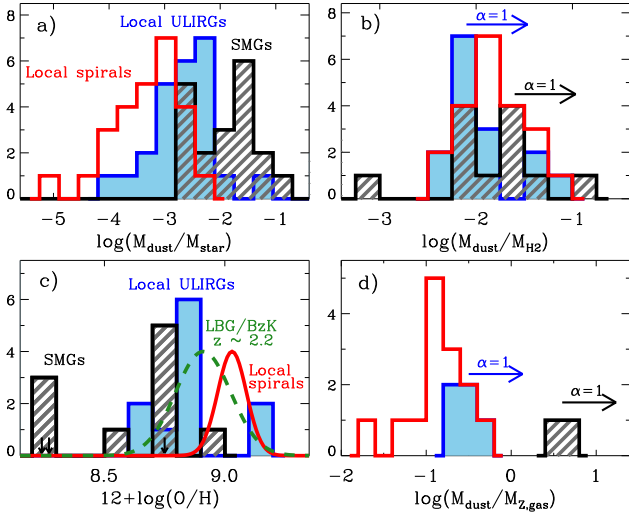


Fig. 2. Panels a), b), d): $M_{\text{dust}}/M_{\text{star}}$, $M_{\text{dust}}/M_{\text{H}_2}$ and $M_{\text{dust}}/M_{\text{Z,gas}}$ distributions, respectively, for high- z SMGs (black hatched), local spirals (SINGS, red open) and local ULIRGs (blue shaded). M_{H_2} is computed adopting $\alpha = 4.3$. Adopting $\alpha = 1$ moves the black and blue histograms by the amount indicated by the arrows. Panel c): metal abundances for the sample of high- z SMGs of Swinbank et al. (2004) (black hatched histogram) and that of local ULIRGs of Rupke et al. (2008) (blue shaded histogram). Submillimeter galaxies in common with our sample are marked by arrows. The red solid and green dashed lines show the metallicity distribution for local spirals (SDSS) and $z \sim 2.2$ star-forming galaxies (Mannucci et al. 2010), respectively, with stellar masses similar to those of our SMGs.

factor $\alpha = 4.3 \text{ M}_\odot (\text{K km s}^{-1} \text{ pc}^2)^{-1}$ for all samples (typically applied to normal spirals) the resulting distribution of $M_{\text{dust}}/M_{\text{H}_2}$ is shown in Fig. 2b, similar for the three samples. If one adopts for ULIRGs and SMGs the conversion factor $\alpha \sim 1 \text{ M}_\odot (\text{K km s}^{-1} \text{ pc}^2)^{-1}$ (thought to be more appropriate for these classes of objects, Solomon & Vanden Bout 2005; Tacconi et al. 2008), then ULIRGs and SMGs have $M_{\text{dust}}/M_{\text{H}_2}$ significantly larger than local spirals, as indicated by the arrows. It is not possible to infer the total gas mass for SMGs by including the fraction of HI, because this is not observed; but similarly to local ULIRGs, the bulk of the gas is probably in the molecular phase (Sanders & Mirabel 1996) in contrast to spirals, which may have a considerable fraction of gas in the atomic phase. As a consequence, by including M_{HI} to obtain the dust-to-total gas ratio, the resulting $M_{\text{dust}}/M_{\text{gas}}$ distribution of ULIRGs and SMGs would be further skewed towards higher values relative to spirals. A dust-to-gas ratio higher than in spirals has also been observed in the central (dense) region of local luminous infrared galaxies (LIRGs) (Wilson et al. 2008). It can possibly be ascribed to enhanced dust production by SNe and by the first generation of AGB stars in young stellar systems (e.g. Michałowski et al. 2010b), and/or to higher accretion of metals on dust grains in these dense environments. In either cases, the finding that the dust-to-gas ratio in SMGs is *not* lower than in local spirals supports the interpretation of their “dust richness” (relative to the stellar mass) in terms of “gas richness”, possibly along with a higher $M_{\text{dust}}/M_{\text{H}_2}$. Summarizing, the high dust content observed in SMGs mirrors their high gas content, the latter with a dust-to-gas ratio similar or higher than normal spiral galaxies.

The latter result is in contrast with the low gas metallicity observed in SMGs though. Indeed, based on their optical nebular lines SMGs have metallicities similar or lower than other strongly star-forming systems, such as ULIRGs in the local Universe (Rupke et al. 2008), as well as Lyman break galaxies (LBGs), BzKs (see Daddi et al. 2004) and ULIRGs at high redshift (Erb et al. 2006; Mannucci et al. 2010; Caputi et al. 2008), which in turn are lower than local, moderately star-forming spirals with the same stellar mass. This is illustrated in Fig. 2c, where the metallicity distribution of different classes of objects was measured with the same method (based on optical nebular lines) and adopting the same metallicity scale as discussed in the Appendix, and within similar stellar mass interval ($M_\star \sim 10^{11} \text{ M}_\odot$). For the SMGs we exploited the sample with rest-frame optical spectroscopy given in Swinbank et al. (2004), which unfortunately overlaps with our sample only for three objects (marked with black arrows). That galaxies with enhanced star formation are characterized by lower metallicity has been noted by various authors (Kewley & Ellison 2008; Rupke et al. 2008; Caputi et al. 2008). Recently Mannucci et al. (2010) showed that the anticorrelation between metallicity and SFR actually accounts for most of the evolution of the mass-metallicity relation at high redshift: high- z galaxies (at least up to $z \sim 2.5$) appear more metal-poor simply because characterized by higher SFRs as a consequence of selection effects. This anticorrelation between SFR and metallicity is ascribed to inflow of metal-poor gas that boosts SF in galaxies. However, the inferred “low” gas metallicities in SMGs are in striking contrast with the high dust content inferred from their far-IR emission.

In Fig. 3 we further investigate this discrepancy by comparing the dust-to-gas ratio with the gas metallicity. Red triangles are all local galaxies for which the complete required information is available; most of the upper limits are due to the lack of detection or of data for the molecular gas. The dotted line shows the trend expected by assuming that the dust content scales linearly with metallicity following the relation (Draine et al. 2007)

$$M_{\text{dust}}/M_{\text{gas}} \approx 0.01 \times (\text{O}/\text{H})/(\text{O}/\text{H})_{\text{MW}}. \quad (1)$$

Actually, Draine et al. (2007) and Hunt et al. (2005) have shown (on a wider sample) that the relation traced by real galaxies is much steeper than expected by Eq. 1, as also hinted by the (much smaller) subset of local spirals/dwarfs shown in Fig. 3. Local ULIRGs (blue symbols) tend to have higher dust-to-gas ratios for a given metallicity, the deviation depending on whether the assumed CO-to- H_2 conversion factor is $\alpha = 1$ (open squares) or $\alpha = 4.3$ (crosses). In the case of SMGs (black symbols) there are only two objects for which the complete required information is available (whose gas metallicity is actually an upper limit), shown both in the case of $\alpha = 1$ (solid squares) and $\alpha = 4.3$ (solid circles). However, it is clear that their dust content is far higher than expected from their metallicity. The HI mass is not included for ULIRGs and SMGs, but the effect is very small (0.1 dex, Sanders & Mirabel 1996). The orange and cyan tracks in Fig. 3 show the expected evolution of the dust content and metallicity as predicted by Calura et al. (2008) for ellipticals and spirals, where it is evident that the large discrepancy observed in SMGs cannot be accounted for by models. In short, in SMGs the mass of metals inferred from the dust content is much larger than the mass of metals inferred from the gas phase.

To further quantify this discrepancy, in Fig. 2d we show the distribution of $M_{\text{dust}}/M_{\text{Z,gas}}$, where $M_{\text{Z,gas}}$ is the mass of metals in the gas phase (i.e. $Z \times M_{\text{gas}}$). We assumed for all objects a conversion factor $\alpha = 4.3$, the arrows showing the effect of using $\alpha = 1$ for ULIRGs and SMGs. Clearly in SMGs $M_{\text{dust}}/M_{\text{Z,gas}}$

is over one order of magnitude higher than in spirals and well above unity. Local ULIRGs share a similar problem, but not as extreme as SMGs. When computing $M_{Z, \text{gas}}$, we assume the same metal abundance for the neutral and ionized gas phases. This can be false, as the former may be characterized by lower (by a factor of ~ 7 , Leboutteiller et al. 2009) abundances than the latter. However, this effect does not change our results. Indeed, dwarf low-metallicity galaxies (see the Appendix), where most of the gas is in the atomic phase, would move towards higher values of $M_{\text{dust}}/M_{Z, \text{gas}}$ by 0.85 dex, while normal spiral galaxies, whose atomic gas fraction is around 50%, would only move by 0.24 dex. The ratio $M_{\text{dust}}/M_{Z, \text{gas}}$ in spiral galaxies and dwarfs would still be lower than in SMGs, where the bulk of the gas is expected to be in the molecular phase (as discussed above).

There are some possible scenarios that could explain this puzzling result. One possibility is that dust masses are erroneously estimated because the dust properties in SMGs are very different from those assumed in our models. The average dust emissivity may be higher. However, this difference would have to be quite dramatic, because the dust masses are off by more than an order of magnitude with respect to those expected by the metallicities. In ULIRGs (extreme starbursts) the emissivity inferred by Clements et al. (2010) is similar to that assumed here.

Another possibility is that as mentioned above the high density in SMGs favors the growth of dust out of metals in the ISM, which also decreases the effective metallicity in the gas phase. However, the standard dust depletion factors in the diffuse ISM are already high, with most metals already locked into dust. Hence, for a given metallicity the dust mass cannot grow by more than a factor of about two through this mechanism.

Finally, the disagreement between the dust content and the gas metallicity can be caused by dust obscuration. Likely, the bulk of the gas in SMGs is metal rich. The associated dust richness and the compact configuration make most of the ISM optically thick at visual wavelengths. As a consequence, the optical nebular lines used to infer the gas metallicity only probe the outer parts of the star-forming regions, which are probably more metal-poor. Paradoxically, the higher metallicity of these dense systems and their associated high dust content may produce the apparent effect of metal-poorness when observed at optical wavelengths. This scenario is supported by the findings of Santini et al. (2009), who showed that luminous IR galaxies have higher mid-IR-based SFR estimates compared to those obtained by correcting the optical-UV light.

If confirmed, the latter two scenarios would not support the current interpretation of the low metallicity observed in ULIRGs and SMGs in terms of inflow of metal-poor gas boosting the star formation (e.g. Montuori et al. 2010). More generally, if the discrepancy between gas and dust metal mass also applies to other populations of high-z starburst galaxies (e.g. BzKs and LBGs) this would prompt a general revision of the interpretation of the apparently low metallicities observed in high-z systems.

Acknowledgements. PACS has been developed by a consortium of institutes led by MPE (Germany) and including UVIE (Austria); KU Leuven, CSL, IMEC (Belgium); CEA, LAM (France); MPIA (Germany); INAF-IFSI/OAA/OAP/OAT, LENS, SISSA (Italy); IAC (Spain). This development has been supported by the funding agencies BMVIT (Austria), ESA-PRODEX (Belgium), CEA/CNES (France), DLR (Germany), ASI/INAF (Italy), and CICYT/MCYT (Spain). This work was supported by ASI through grant I/005/07/0.

References

Berta et al. 2010, A&A, Special Issue
Bothwell, M. S., Chapman, S. C., Tacconi, L., et al. 2009, ArXiv e-prints
Calura, F., Pipino, A., & Matteucci, F. 2008, A&A, 479, 669

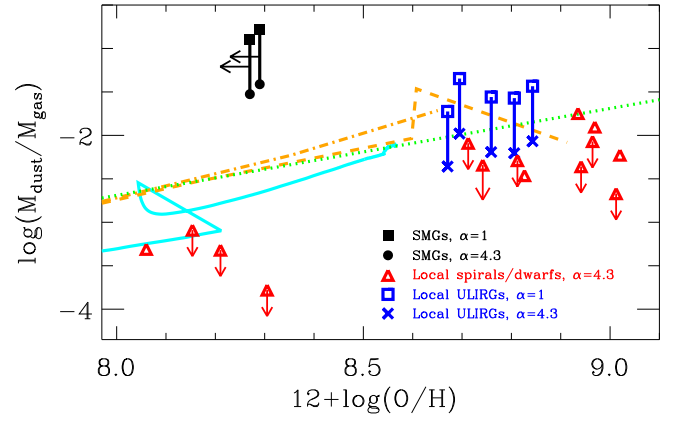


Fig. 3. Dust-to-gas ratio versus metallicity. The black and blue symbols show high-z SMGs and local ULIRGs, respectively, by assuming different conversion factors as indicated by the legend. Red triangles refer to local spirals. The green dotted line shows the trend expected by Eq. 1. The solid cyan and dashed (dot-dashed) orange lines show the evolutionary tracks predicted by the model of Calura et al. (2008) for spirals and proto-ellipticals with mass of 10^{11} (10^{12}) M_{\odot} .

- Caputi, K. I., Lilly, S. J., Aussel, H., et al. 2008, ApJ, 680, 939
Chapman, S. C., Blain, A. W., Smail, I., & Ivison, R. J. 2005, ApJ, 622, 772
Clements, D. L., Dunne, L., & Eales, S. 2010, MNRAS, 403, 274
Daddi, E., Cimatti, A., Renzini, A., et al. 2004, ApJ, 617, 746
Daddi, E., Dannerbauer, H., Stern, D., et al. 2009, ApJ, 694, 1517
Dale, D. A., Gil de Paz, A., Gordon, K. D., et al. 2007, ApJ, 655, 863
Draine, B. T., Dale, D. A., Bendo, G., et al. 2007, ApJ, 663, 866
Draine, B. T. & Li, A. 2007, ApJ, 657, 810
Dunne, L., Eales, S. A., & Edmunds, M. G. 2003, MNRAS, 341, 589
Erb, D. K., Shapley, A. E., Pettini, M., et al. 2006, ApJ, 644, 813
Evans, A. S., Mazzarella, J. M., Surace, J. A., & Sanders, D. B. 2002, ApJ, 580, 749
Fontana, A., Salimbeni, S., Grazian, A., et al. 2006, A&A, 459, 745
Greve, T. R., Bertoldi, F., Smail, I., et al. 2005, MNRAS, 359, 1165
Hughes, D. H., Serjeant, S., Dunlop, J., et al. 1998, Nature, 394, 241
Hunt, L., Bianchi, S., & Maiolino, R. 2005, A&A, 434, 849
Kennicutt, Jr., R. C. 1992, ApJ, 388, 310
Kennicutt, Jr., R. C., Armus, L., Bendo, G., et al. 2003, PASP, 115, 928
Kewley, L. J. & Ellison, S. L. 2008, ApJ, 681, 1183
Kneib, J., Neri, R., Smail, I., et al. 2005, A&A, 434, 819
Knudsen, K. K., Neri, R., Kneib, J., & van der Werf, P. P. 2009, A&A, 496, 45
Kovács, A., Chapman, S. C., Dowell, C. D., et al. 2006, ApJ, 650, 592
Leboutteiller, V., Kunth, D., Thuan, T. X., & Désert, J. M. 2009, A&A, 494, 915
Li, A. & Draine, B. T. 2001, ApJ, 554, 778
Magnelli et al. 2010, A&A, Special Issue
Maiolino, R., Nagao, T., Grazian, A., et al. 2008, A&A, 488, 463
Mannucci, F., Cresci, G., Maiolino, R., Marconi, A., & Gnerucci, A. 2010, ArXiv e-prints
Michałowski, M., Hjorth, J., & Watson, D. 2010a, A&A, 514, A67+
Michałowski, M. J., Watson, D., & Hjorth, J. 2010b, ApJ, 712, 942
Miller, B. W. 1996, AJ, 112, 991
Miller, B. W. & Hodge, P. 1996, ApJ, 458, 467
Montuori, M., Di Matteo, P., Lehnert, M. D., Combes, F., & Semelin, B. 2010, ArXiv e-prints
Moustakas, J. & Kennicutt, R. C. J. 2007, VizieR Online Data Catalog, 216, 40081
Nagao, T., Maiolino, R., & Marconi, A. 2006, A&A, 459, 85
Omukai, K., Tsuribe, T., Schneider, R., & Ferrara, A. 2005, ApJ, 626, 627
Papadopoulos, P. P., van der Werf, P., Isaak, K., & Xilouris, E. M. 2010, ArXiv e-prints
Pilbratt et al. 2010, A&A, Special Issue
Poglitsch et al. 2010, A&A, Special Issue
Pope, A., Scott, D., Dickinson, M., et al. 2006, MNRAS, 370, 1185
Rupke, D. S. N., Veilleux, S., & Baker, A. J. 2008, ApJ, 674, 172
Sanders, D. B. & Mirabel, I. F. 1996, ARA&A, 34, 749
Sanders, D. B., Scoville, N. Z., & Soifer, B. T. 1988, ApJ, 335, L1
Sanders, D. B., Scoville, N. Z., & Soifer, B. T. 1991, ApJ, 370, 158
Santini, P., Fontana, A., Grazian, A., et al. 2009, A&A, 504, 751

- Schurer, A., Calura, F., Silva, L., et al. 2009, MNRAS, 394, 2001
Silva, L., Granato, G. L., Bressan, A., & Danese, L. 1998, ApJ, 509, 103
Solomon, P. M., Downes, D., Radford, S. J. E., & Barrett, J. W. 1997, ApJ, 478, 144
Solomon, P. M. & Vanden Bout, P. A. 2005, ARA&A, 43, 677
Swinbank, A. M., Smail, I., Chapman, S. C., et al. 2004, ApJ, 617, 64
Tacconi, L. J., Genzel, R., Smail, I., et al. 2008, ApJ, 680, 246
Wilson, C. D., Petitpas, G. R., Iono, D., et al. 2008, ApJS, 178, 189
Yan, L., Tacconi, L., Fiolet, N., et al. 2010, ArXiv e-prints

Appendix A: Authors affiliations

- ¹ INAF - Osservatorio Astronomico di Roma, via di Frascati 33, 00040 Monte Porzio Catone, Italy.
- ² Max-Planck-Institut für Extraterrestrische Physik (MPE), Postfach 1312, 85741 Garching, Germany.
- ³ INAF-Osservatorio Astronomico di Trieste, via Tiepolo 11, 34131 Trieste, Italy.
- ⁴ Herschel Science Centre; European Space Astronomy Centre.
- ⁵ ESO, Karl-Schwarzschild-Str. 2, D-85748 Garching, Germany.
- ⁶ Laboratoire AIM, CEA/DSM-CNRS-Université Paris Diderot, IRFU/Service d'Astrophysique, Bât.709, CEA-Saclay, 91191 Gif-sur-Yvette Cedex, France.
- ⁷ Instituto de Astrofísica de Canarias, 38205 La Laguna, Spain.
- ⁸ Departamento de Astrofísica, Universidad de La Laguna, Spain.
- ⁹ Department of Astronomy, 610 Space Sciences Building, Cornell University, Ithaca, NY 14853, USA.
- ¹⁰ Jeremiah Horrocks Institute for Astrophysics and Supercomputing, University of Central Lancashire, Preston PR1 2HE, UK.
- ¹¹ Dipartimento di Astronomia, Università di Bologna, Via Ranzani 1, 40127 Bologna, Italy.
- ¹² INAF-Osservatorio Astronomico di Bologna, via Ranzani 1, 40127 Bologna, Italy.
- ¹³ INAF-IFSI, Via Fosso del Cavaliere 100, 00133 Roma, Italy.
- ¹⁴ Dipartimento di Astronomia, Università di Trieste, via G. B. Tiepolo 11, 34143 Trieste, Italy.
- ¹⁵ Dipartimento di Astronomia, Università di Padova, Vicolo dell'Osservatorio 3, 35122 Padova, Italy.

Appendix B: Ancillary data

Here we first describe the ancillary data used for SMGs (stellar mass, gas mass and metallicity) and afterwards the local samples used for comparison.

B.1. Submillimeter galaxies

Stellar masses of SMGs are computed by fitting the optical-to-near-IR photometry compiled by the PEP Team to synthetic models, which is fully described in Fontana et al. (2006), fixing the redshifts to those of the SMGs. For consistency with the theoretical models of Calura et al. (2008) with which we compare our results, we adopt a Scalo IMF, which implies stellar masses higher than those calculated assuming a Salpeter IMF by a factor 1.15.

When possible, we obtained information on the gas mass. For the SMG sample we were able to find CO millimetric data for 12 galaxies (the three measurements of the triple image of the lensed galaxy in Abell2218 are counted once) (Bothwell et al. 2009; Kneib et al. 2005; Daddi et al. 2009; Greve et al. 2005; Knudsen et al. 2009). To derive the molecular gas masses we followed the prescriptions given in the associated references, but we normalized them to the same CO-to-H₂ conversion factor. In particular we show the results assuming (conservatively) a CO-to-H₂ conversion factor $\alpha = 4.3 \text{ M}_\odot (\text{K km s}^{-1} \text{ pc}^2)^{-1}$, which applies to normal spirals; but we also show the effect of assuming $\alpha = 1 \text{ M}_\odot (\text{K km s}^{-1} \text{ pc}^2)^{-1}$, which is thought to be more appropriate for ULIRGs and SMGs (Solomon et al. 1997; Tacconi et al. 2008).

We inferred the gas metallicities through the optical nebular line emission by using the strong-line methods. Within this context, and especially when comparing different samples, it is most important to use consistent (inter-)calibrations and, if possible, use the same diagnostic emission line ratios. Here we adopted the calibrations obtained by Nagao et al. (2006) and refined by Maiolino et al. (2008), who inter-calibrate all strong line diagnostics to the same scale. For the SMGs we used as metallicity diagnostic the ratio [NII]/H α given in Swinbank et al. (2004). An AGN may easily affect the nebular line ratios and make them deviate from the metallicity calibration for star-forming galaxies. For this reason we removed targets classified as AGNs in Swinbank et al. (2004). We also removed one object with [NII]/H α = 0.65, because such a high ratio is only observed in AGNs or shocked regions. In total, we obtain gas metallicities for a sample of 10 SMGs, three of which also belong to our SMG sample with dust masses. The [NII]/H α ratio of these objects may still be affected by an unrecognized AGN, but this would make our results conservative, because the contribution by an unrecognized AGN would make the gas metallicity apparently higher than its actual value.

B.2. Local galaxies

To compare the dust content in high redshift SMGs with normal and actively star-forming galaxies in the local Universe, we assembled two sets of data:

- a sample of 26 local spirals out of the SINGS sample (Kennicutt et al. 2003; Dale et al. 2007; Draine et al. 2007) with full multi-wavelength photometry and also with submm data for a proper dust mass measurement;
- a sample of 24 local ULIRGs taken from the Clements et al. (2010) sample with at least three submm photometric points. Optical and near-IR fluxes needed to compute the stellar mass of these galaxies were collected from public archives.

Stellar masses were inferred by the same method and IMF as SMGs.

For the local spirals, we took the HI and H₂ mass estimates from Kennicutt et al. (2003), while for the ULIRGs we collected H₂ mass estimates from Sanders et al. (1988), Sanders et al. (1991), Solomon et al. (1997), Evans et al. (2002) and Papadopoulos et al. (2010). Here we also assumed a CO-to-H₂ conversion factor $\alpha = 4.3 \text{ M}_\odot (\text{K km s}^{-1} \text{ pc}^2)^{-1}$, but for ULIRGs we also show the effect of assuming $\alpha = 1 \text{ M}_\odot (\text{K km s}^{-1} \text{ pc}^2)^{-1}$.

Concerning the gas metallicity in the local spiral sample, there are only a few objects (six after removing possible AGN-dominated galaxies) out of the SINGS sample with submm data that also have integrated spectroscopy (Moustakas & Kennicutt 2007; Kennicutt 1992), which could be used to infer the gas metallicity with the same strong line method and calibration scale adopted for SMGs. For these objects we also exploited the diagnostics involving [OII]3727, [OIII]5007 and H β , which help to better constrain the metallicity along with [NII]/H α , while they are still fully consistent with the global inter-calibrations presented in Maiolino et al. (2008). Draine et al. (2007) uses the metallicities for a more extended set of SINGS galaxies, but by adopting different calibrations, which therefore cannot be used for direct comparison with the SMGs. To expand the sample of objects with dust masses *and* metallicity (especially in the low-metallicity range), we included nine dwarf and spiral galaxies of the SINGS sample without submm photometry

(Draine et al. 2007). There the M_{dust} estimates were taken from Draine et al. (2007) (whose dust masses are consistent with ours for the objects in common, as discussed in the text), and their integrated emission line fluxes, which were required to place them in the same metallicity scale as SMGs and ULIRGs, were collected from Moustakas & Kennicutt (2007), Miller & Hodge (1996) and Miller (1996).

For the ULIRGs we collected spectroscopic data from Rupke et al. (2008). We removed galaxies classified as AGNs based on the diagnostic diagrams.

In order to have a more comprehensive statistic (only 6 out of the 26 local spirals from the SINGS sample have integrated spectroscopy which can be used to compute their metal abundance), the metallicity distribution of local spirals shown by the red, solid line in Fig. 2c is obtained from the large SDSS sample presented in Kewley & Ellison (2008) in the same mass range as SMGs and ULIRGs, with the same metallicity calibrations and scale used in Maiolino et al. (2008), i.e. consistent with the other samples. The metallicity distribution of LBGs and BzKs at $z \sim 2.2$ (with $\log M_{\star} \sim 10.6 M_{\odot}$) is taken from Mannucci et al. (2010), who adopt the same scale and calibrations as Maiolino et al. (2008).